

## **A multiscale framework for lubrication analysis of bearings with textured surface**

\*Leiming Gao<sup>1)</sup>, Gregory de Boer<sup>2)</sup> and Rob Hewson<sup>3)</sup>

<sup>1), 3)</sup> *Aeronautics Department, Imperial College London, London, SW7 2AZ, UK*

<sup>2)</sup> *School of Mechanical Engineering, University of Leeds, Leeds, LS2 9JT, UK*

<sup>1)</sup> [leiming.gao@gmail.com](mailto:leiming.gao@gmail.com)

### **ABSTRACT**

In this paper a heterogenous multiscale method is applied to model the Elastohydrodynamic Lubrication (EHL) problem with small scale topographical features. The small scale fluid-structure interaction (FSI) model couples both the fluid flow between the bearing surfaces and the elastic deformation of the solid bearing material. The large scale geometry is a 2D cylinder line contact for journal bearings of the order of a centimeter in size, and the small scale topography is a uniformly distributed pocket of the order of micrometers in size. In the results, the effects of topographical features on the bearing's lubrication and friction performance are presented and the importance of the role of cavitation at the small scale feature is highlighted.

**KEYWORDS:** Bearing Surface Texture, Heterogenous Multiscale Method, Fluid Structure Interaction

### **1. INTRODUCTION**

In engineering, bearings benefit from a full fluid film between the two bearing surfaces, so that the bearing can sustain load with low friction and wear by avoiding solid-solid contacts. At high loads the pressures result in a deformation of the bearing surface, resulting in EHL (Hamrock 1994), such a change in the geometry consequently changes the fluid domain and the fluid pressure.

Surface texture has gained increasing interest in bearings recently (de Kraker 2007, Sahlin 2007 and Hewson 2011), with experimental investigations showing that changes to the bearing surface can lead to an improved load carrying capacity and low friction (Etsion 1999). The size of bearing surface topography and that of bearing itself are generally in different order of magnitudes presenting a challenge to the deterministic numerical simulation.

In this paper a heterogenous multiscale method (E 2003 and Gao 2012) is introduced to the numerical analysis of the EHL, with the influence of micro-topological features highlighted. This numerical model couples the fluid flow between the bearing surfaces, and the elastic deformation of the solid at two scales. As the explicit

---

<sup>1)</sup> Postdoctoral Research Fellow

<sup>2)</sup> Ph.D. Student

<sup>3)</sup> Senior Lecturer

governing equation of fluid flow, the pressure gradient and mass flow rate relationship, is obtained from a homogenised small scale solution, along with consideration of the local deformation of the bearing surface. While the non-local deformation of the bearing surface is considered at the large scale. This relationship is subsequently used to solve the global pressure in the large scale simulation. The small scale simulation accounts for the micro flow and local deformations in a unit surface cell. The Navier-Stokes equations, together with the interaction with the solid bearing are solved using the Finite Element package (COMSOL Multiphysics). Fluid cavitation is considered at the small scale within this work, via a predefined threshold cavitation pressure (Sahlin 2007). The fluid is assumed a mixture of liquid and vapour whose density varies depending on pressure. This approach and the local cavitation model raises some interesting questions regarding the near-periodic assumptions underlying the Heterogeneous Multiscale Method.

## 2. NUMERICAL METHODOLOGY

### 2.1 Heterogeneous Multiscale Method (HMM)

HMM is a general technique that has been applied to a number of problems where there is a distinct separation of scales (E 2003). It assumes that the large scale model is known, in which some terms are explicitly unknown, and chooses a conventional large scale solver as the starting point. In the process of implementing this large scale solver, small scale numerical simulations are used to replace function evaluations that involve unknown quantities. The key to the application of the HMM approach proposed here is how the two scales are coupled.

For this particular application, the small scale results provide the homogenised pressure gradient-mass flow rate relationship, while the large scale applies this solution via a global pressure distribution and conservation of mass. The bearing surface deformation is considered at both scales, local scale as part of the FSI solution and the large scale due to non-local deformations of the problem.

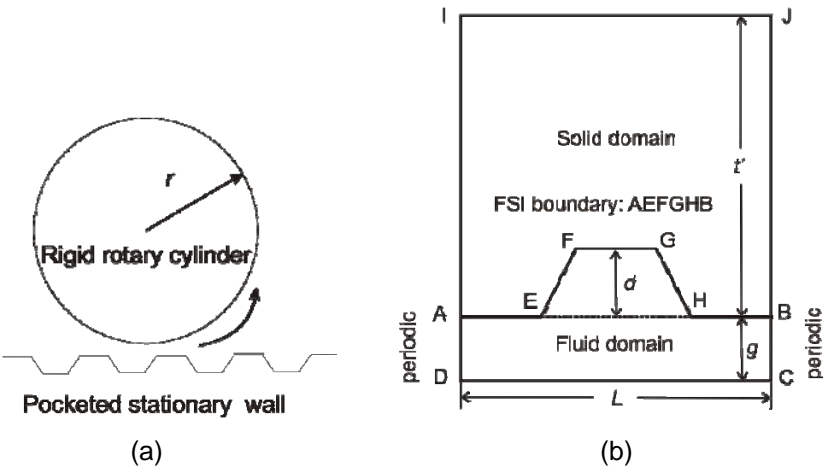


Fig. 1 (a) Global geometry of the cylinder bearing in line contact; (b) micro pocket geometry of a unit cell on the stationary wall surface.

## 2.2 Geometry and Materials

The global geometry of the lubrication model is a 2D cylinder bearing in line contact. The cylinder is assumed to rotate with ideal smooth surface and the plane is stationary with micro-pocket surface textures, as shown in Fig. 1. The material of cylinder is assumed to rigid and that of the plane is linearly elastic with Young's modulus of 0.5 GPa and Poisson's ratio of 0.4. The radius of the cylinder ( $r$ ) is 25 mm and the corresponding sliding speed ( $U$ ) is 2 m/s. The micro-pocket length ( $L$ ) ranges between 20  $\mu\text{m}$  and 200  $\mu\text{m}$  and the depth ( $d$ ) between 5  $\mu\text{m}$  and 30  $\mu\text{m}$ .

## 2.3 Large Scale Simulation

The large scale simulation describes the fluid-structure interaction in the global lubrication domain, where the fluid pressure are solved simultaneously with the bearing elastic deformation. The difference between the current study and classic EHL is that the governing equation for pressure is a homogenised equation from the small scale simulations, rather than the Reynolds equation, expressed as

$$\frac{dp}{dx} = f(g, p, q) \quad (1)$$

$$\frac{dq}{dx} = 0 \quad (2)$$

The pressure gradient ( $\frac{dp}{dx}$ ) is a homogenised function of the cell inlet pressure ( $p$ ), mass flow rate ( $q$ ) and locally undeformed gap ( $g$ ). The three parameters ( $p$ ,  $g$ ,  $q$ ) in the right-hand-side of Eq. (1) are the only large-scale-derived parameters that influence the small scale flow. The large scale boundary conditions used to solve Eqs. (1) and (2) is that the pressure at the global inlet and outlet boundaries is equal to zero

$$p_{\text{in}} = p_{\text{out}} = 0 \quad (3)$$

Once the pressure distribution is obtained, the bearing load is calculated as

$$w = \int_{x_{\text{in}}}^{x_{\text{out}}} p \, dx \quad (4)$$

The shear stress ( $\tau$ ) distribution is obtained through interpolation of corresponding small scale shear stress and the friction coefficient ( $\mu$ ) is calculated as

$$\mu = \frac{\int_{x_{\text{in}}}^{x_{\text{out}}} \tau \, dx}{w} \quad (5)$$

## 2.4 Small Scale Simulations

The small scale problem is described by the flow equations and those governing the elastic deformation of the small scale features. The coupling is facilitated through the application of the Arbitrary Lagrangian Eularian (ALE) method (COMSOL

Multiphysics).

The isothermal, laminar flow is governed by the compressible Navier-Stokes equations.

$$\rho(\mathbf{u} \cdot \nabla)\mathbf{u} = \nabla \cdot [-p\mathbf{I} + \eta(\nabla\mathbf{u} + (\nabla\mathbf{u})^T) - 2\eta/3(\nabla \cdot \mathbf{u})\mathbf{I}] \quad (6)$$

$$\nabla \cdot (\rho\mathbf{u}) = 0 \quad (7)$$

with  $\rho$  denotes the fluid density,  $\mathbf{u}$  the velocity vector,  $p$  the fluid pressure,  $\eta$  the fluid viscosity,  $\mathbf{I}$  the unit tensor. The boundary conditions are shown in Fig. 1(b). The lower boundary CD (Fig. 1(b)) is a sliding wall. The upper fluid structure interface is a no slip boundary. Near-periodic boundary conditions apply on the AD and BC boundary in terms of mass flow rate (product of velocity and density) scaled by local strain due to small scale deformation and a uniform pressure jump,  $\Delta p$ .

In the solid domain in Fig. 1(b), a plain strain model is applied. The strain-stress relationship is described by the following equations

$$\varepsilon_x = \frac{1-\nu^2}{E} \left( \sigma_x - \frac{\nu}{1-\nu} \sigma_y \right) \quad (8)$$

$$\varepsilon_y = \frac{1-\nu^2}{E} \left( \sigma_y - \frac{\nu}{1-\nu} \sigma_x \right) \quad (9)$$

where  $\sigma$  is normal stress. The top boundary IJ is fully constrained. The vertical boundary AI and BJ is constrained in the  $x$  (normal) direction only. The FSI boundary (marked in Fig. 1(b)) is free and subject to the fluid pressure. The equivalent local pressure  $p$  to represent the unit cell pressure is defined as the average pressure across the cell

$$p = \frac{\int_0^L p \, dx}{L} \quad (10)$$

Details can be found in Gao (2012).

### 2.5 Separation of the Deformation Coefficient Matrix

The bearing surface deformation is expressed as

$$\boldsymbol{\delta} = \mathbf{K} \times \mathbf{p} \quad (11)$$

The displacement influence coefficient matrix ( $\mathbf{K}$ ) is a  $n$ -by- $n$  matrix where  $n$  is the number of large scale mesh grid. The diagonal terms and non-diagonal terms are separated from the total deformation matrix that

$$\mathbf{K} = \mathbf{K}_1 + \mathbf{K}_2 \quad (12)$$

where, diagonal matrix ( $\mathbf{K}_1$ ) is composed of all diagonal elements of the total coefficient

matrix ( $\mathbf{K}$ ). Physically its element  $K_{ij}$  means the displacement at point  $i$  due to a unit local pressure  $p_i$  (i.e. load per unit length for line contacts). The non-diagonal matrix ( $\mathbf{K}_2$ ) is the total coefficient matrix ( $\mathbf{K}$ ) with the diagonal elements removed. Physically its elements  $K_{ij}$  define the displacement at point  $i$  due to non-local  $p_j$  (for  $j \neq i$ ). So that the total deformation in Eq. (11) are accounted for separately at both scales

$$\boldsymbol{\delta} = \mathbf{K}_1 \times \mathbf{p} + \mathbf{K}_2 \times \mathbf{p} \quad (13)$$

The non-diagonal terms ( $\mathbf{K}_2 \times \mathbf{p}$ ) account for the non-local large scale deformation. The diagonal terms ( $\mathbf{K}_1 \times \mathbf{p}$ ) account for the local deformation.

Since a small scale feature is regarded as a point at the large scale, the local deformation is assumed as a spring column (as described by the deformation matrix). Thus, an equivalent height of the solid domain ( $t'$ ) is introduced in order to ensure that the local deformation in the small scale simulations is the same as the column deformation obtained from the diagonal matrix  $\mathbf{K}_1$ .

$$t' = k_1 \times E' \quad (14)$$

where,  $k_1$  represents the elements in matrix  $\mathbf{K}_1$ .  $E'$  is the equivalent elastic modulus, for the plain strain model

$$E' = \frac{(1-\nu)E}{(1+\nu)(1-2\nu)} \quad (15)$$

where  $E$  and  $\nu$  is the Young's modulus and Poisson's ratio of the bearing material respectively. The local deformation calculated using the equivalent material height  $t'$  is consistent with the diagonal terms  $\mathbf{K}_1 \times \mathbf{p}$  in Eq. (13).

## 2.6 Cavitation Model

The lubricant is assumed to a mixture of liquid and gas<sup>[6]</sup>. When the fluid pressure drops below certain saturation pressure (zero in the current study) cavitation occurs that some gas resolved in the fluid will comes out. The threshold cavitation pressure is defined as  $-0.03$  MPa. The fraction of the liquid and gas mixture is defined through the inverse tangent function

$$\alpha = 0.5 \times \left(1 + \tan^{-1} \frac{p+2 \times 10^4}{10^4}\right) \quad (16)$$

So that the viscosity and density of the mixture is expressed as

$$\eta = \max(10^{-5}, \eta_0 \times \alpha) \quad (17)$$

$$\rho = \max(0.1, \rho_0 \times \alpha) \quad (18)$$

where,  $\eta_0$  and  $\rho_0$  are the viscosity and density of Newtonian fluid with values chosen as  $0.1$  Pa s and  $870$  kg/m<sup>3</sup> respectively.

### 3. RESULTS AND DISCUSSION

The variables are transformed to the non-dimensional forms for convenience of numerical computing, in small scale simulations

$$G = \frac{g}{L}, P = \frac{pL}{\eta_0 U}, Q = \frac{q}{\rho_0 L U}, \frac{dP}{dX} = \frac{dp}{dx} \cdot \frac{L^2}{\eta_0 U} \quad (19)$$

At the large scale  $x$  is non-dimensionalized by the Herzian line contact radius

$$X = x / \sqrt{\frac{8wr}{\pi E}} \quad (20)$$

The load is fixed to 2500 N in the current study for all cases. The large scale calculation domain is  $X = [-4, 2]$ , and the number of mesh point  $n = 120$ .

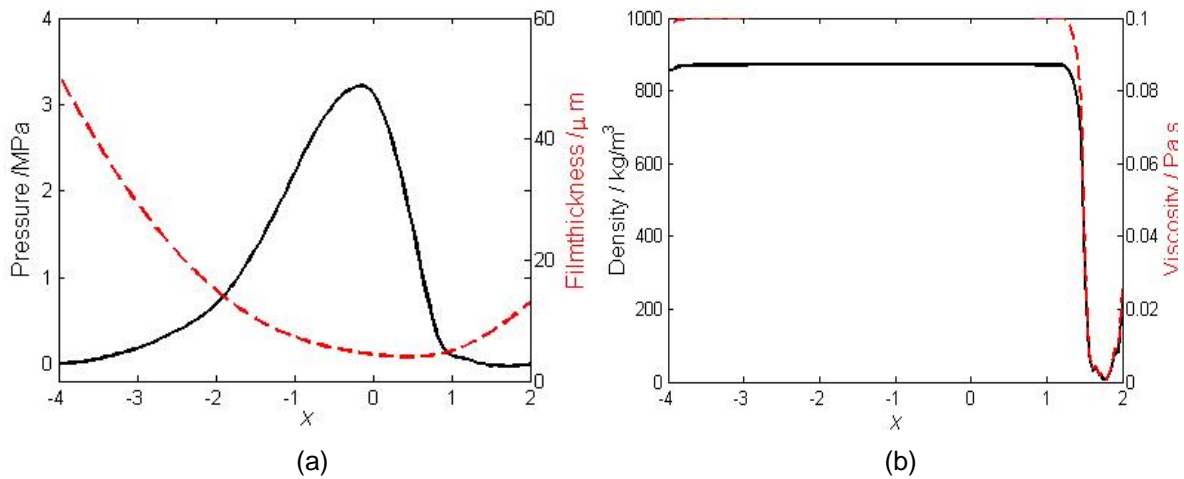


Fig. 2 (a) The large scale fluid pressure and film thickness distributions;  
(b) The large scale viscosity and density variation. ( $L = 200 \mu\text{m}$ ,  $d = 20 \mu\text{m}$ )

The large scale solutions in terms of pressure, film thickness and fluid viscosity and density are the average value of the corresponding local small scale simulations. The fluid pressure and film thickness distributions at the large scale are shown in Fig. 2(a), with cell length of  $200 \mu\text{m}$  and depth  $20 \mu\text{m}$ . The large scale gap deforms from the unloaded geometry with a flattened region in the middle of contact under a maximum pressure of 3.1 MPa. The average viscosity and density variations at large scale are plotted in Fig. 2(b). The large scale cavitation occurs at the outlet boundary of the global flow, where the average density of the mixture drops from a liquid density down to nearly a gas density, so does the viscosity. If we look at this cavitation zone at the small scale, the variations of pressure and density (or viscosity) fraction in the pocket

cell at six local positions are presented in Fig. 3. The pressure drops gradually along the global flow direction starting from around 0.2 MPa (equivalent local pressure) down to the cavitation pressure of  $-0.03$  MPa. Since the small scale pocket itself is a diverge-converge geometry the pressure drops firstly at the diverged edge and then transfers to the converged edge. It is interesting to note that at some locations the large scale average pressure is still positive but cavitation occurs at the small scale; for example, at  $X = 0.9$  (red) and  $0.95$  (green), the large scale pressure is above zero and the average density (or viscosity) has not dropped yet (as seen in Fig. 2(b), while the small scale pressure drops down to  $-0.02$  MPa and the fluid density drops to about 30-40% of that of full liquid fluid, as shown in Fig. 3.

The friction coefficient and minimum film thickness are presented with different cell depth to length ratio in Fig. 4. For short cell length  $20 \mu\text{m}$  and  $50 \mu\text{m}$  the friction

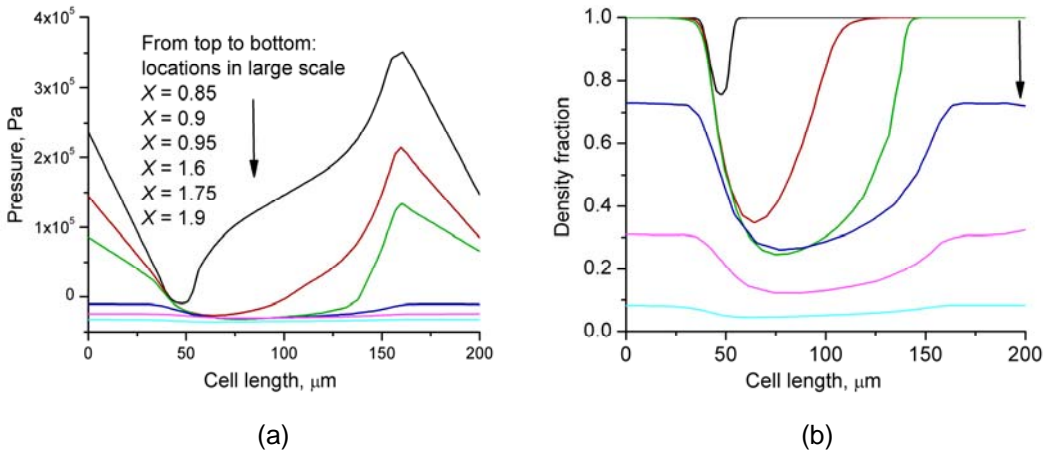


Fig. 3 Small scale pressure (a) and density fraction; (b) variations at different local points near the large scale outlet zone

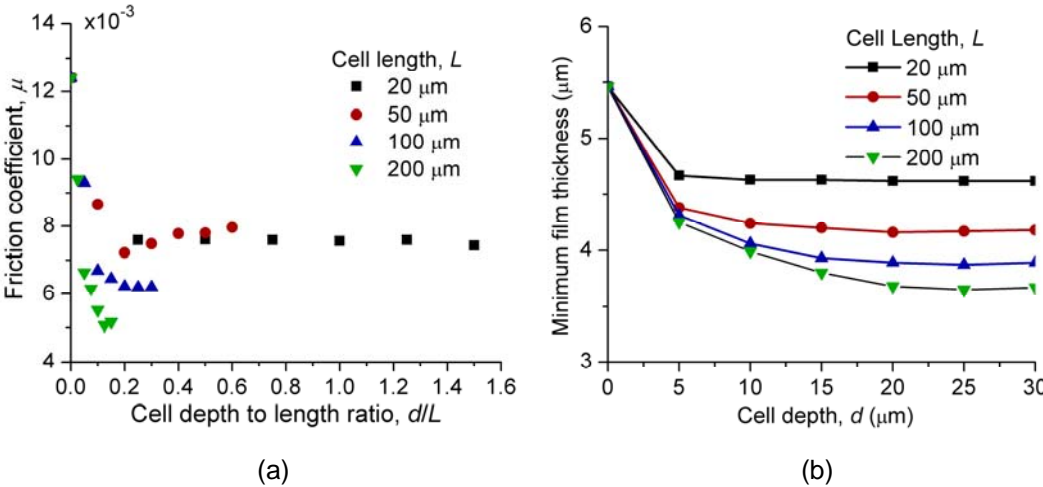


Fig. 4 (a) The friction coefficient ( $\mu$ ) against the cell depth to length ratio; (b) The minimum film thickness against cell depth

coefficient seems to depend on the cell depth to length ratio and the ratio above 0.2 provides lower friction coefficient. While for large cell length 100  $\mu\text{m}$  and 200  $\mu\text{m}$  it seems that the deeper cell results in the lower friction coefficient. The film thickness is reduced in bearings with textured surface and the larger cell length results in the smaller minimum film thickness.

#### 4. CONCLUSIONS

A heterogeneous multiscale model is developed for the fluid-structure interaction in bearing lubrication with the bearing surface texture addressed. The full Navier-Stokes equations together with local elastic deformations are solved at the small scale. The elastic deformation of the bearing surface is considered at both the large and small scales, by decomposing the deformation influence matrix into the diagonal terms and non-diagonal terms (resolved at the small scale and large scale respectively). A pressure gradient and mass flow rate relationship links the two scales, which is homogenised via interpolation of the data from small scale solutions, and applies to the large scale domain.

Fluid cavitation is numerically simulated via a predefined function of the fluid density and pressure. It is explicitly modelled at the small and large scales, whereas it is only modelled at the small scale – the results of which pass to the large scale. The cavitation's development at the large scale outlet zone is presented. It is observed that cavitation occurs at the small scale when the large scale equivalent pressure is still positive.

The friction performance is compared for different small scale geometries. It is observed that a large cell depth results in a low friction coefficient and also a low film thickness. For a journal bearing low friction coefficient is advantageous, however a small film thickness is often unwanted as it would reduce the boundary between the low friction EHL regime and that of the higher friction and wear mixed or boundary lubrication regime. The multiscale method described in the current study provides an approach that can be implemented in the optimization of the geometry of small scale features for bearing lubrication and potentially other FSI applications. The current multiscale model is in 2D and will be fully developed to 3D in our future work.

#### ACKNOWLEDGEMENTS

The authors would like to thank the Leverhulme Trust for the financial support to this work.

#### REFERENCES

- Hamrock B.J. (1994), *Fundamentals of Fluid Film Lubrication*, McGraw-Hill, New York.
- de Kraker, A., Ostayen, R., Beek, A., and Rixen, D. (2007), "A Multiscale Method Modelling Surface Texture Effects", *Trans. ASME Jour. of Trib.*, **129**(2), 221-230.

- Sahlin, F., Almqvist, A., Larsson, R., and Glavatskih, S. (2007), "Rough Surface Flow Factors in Full Film Lubrication Based on a Homogenization Technique", *Trib. Int.*, **40**(7), 1025-1034.
- Hewson, R., Kapur, N., and Gaskell, P. (2011), "A Two-Scale Model for Discrete Cell Gravure Roll Coating", *Chem. Eng. Sci.*, **66**(16), 3666-3674.
- Etsion, I., Kligerman, Y., and Halperin, G. (1999), "Analytical and Experimental Investigation of Laser-Textured Mechanical Seal Faces", *Trib. Trans.*, **42**(3), 511–516.
- E, W., Engquist, B. and Huang Z. (2003), "Heterogeneous Multi-Scale Methods: A General Methodology for Multiscale Modelling", *Phys. Review B*, **67**(9), 092101.
- Gao, L and Hewson, R. (2012), "A Multiscale Framework for EHL and Micro-EHL", *Trib. Trans.* **55**(6), 713-722.
- COMSOL Multiphysics (2008), *User's Guide v3.5a*, COMSOL Ltd.